Combustion Diagnostics by Means of Multizone Heat Release Analysis and NO Calculation

Egnell, Rolf

Published in:
SAE technical paper series

1998

SAE TECHNICAL PAPER SERIES

981424

Combustion Diagnostics by Means of Multizone Heat Release Analysis and NO Calculation

Rolf Egnell
Lund Institute of Technology

The Engineering Society For Advancing Mobility Land Sea Air and Space®
INTERNATIONAL

International Spring Fuels and Lubricants Meeting and Exposition
Dearborn, Michigan
May 4-6, 1998

400 Commonwealth Drive, Warrendale, PA 15096-0001 U.S.A. Tel: (724) 776-4841 Fax: (724) 776-5760

ISSN 0148-7191

Printed in USA

981424

Combustion Diagnostics by Means of Multizone Heat Release Analysis and NO Calculation

Rolf Egnell
Lund Institute of Technology

ABSTRACT

In this paper a combustion diagnostic method is presented where measured pressure data is used to calculate the heat release, local temperatures and concentrations of NO and other species. This is done by a multizone model where the lambda value, i.e. 1/equivalence ratio, in each zone can be chosen arbitrarily. In homogenous charge engines lambda is given by the global air/fuel ratio. The local lambdas during initial combustion in stratified charge and diesel engines have to be estimated either as an average value or with a chosen distribution.

One new zone of each local lambda is generated and the temperature, volume and species in all old zones are updated at each time step of calculation. In this paper the model is demonstrated by using pressure data from premixed and direct injected stratified charge natural gas SI engines and from a DI diesel engine.

The pre-mixed data is used to validate the model as such while the ambition in the stratified charge and diesel cases has been to find the average local lambda that gives the same NOx emission as measured. The emphasis in the latter cases has been to study the influence on average local lambda of the duration of the fuel injection. Early injected fuel seems to burn at slightly leaner mixtures than later injected.

INTRODUCTION

The chemistry responsible for NOx formation in internal combustion engines has been thoroughly investigated by many researchers. Experimental data have verified that the so-called Zeldovich mechanism is the main source of NO emissions. Thus any difference in NO emissions from different types of IC engines and load conditions can be attributed to the local environment influencing the reactions in this specific mechanism.

The concentration of NO and other species in the exhausts reflect the conditions under which the fuel was burnt in the cylinder. Products from combustion like CO_2, CO, H_2, H_2O, O_2, N_2 and unburned fuel give information of global quantities like the air/fuel ratio (AFR) and the combustion efficiency. Due to the strong temperature dependence of the Zeldowich mechanism, the reactions involving NO freeze early during the expansion stroke, which means that the local conditions in the cylinder at that time have a major influence on the emissions of NO.

In the work presented in this paper the measured concentration of NOx is used as a diagnostic tool in order to, at least qualitatively, investigate the local conditions in the cylinder of different types of engines and load conditions. For this purpose a multizone model for combustion and NO formation has been developed.

Inputs to the model are measured emissions of CO_2, CO, O_2 , NOx, total hydrocarbons (THC) and crank angle resolved cylinder pressure. Also needed are the temperature and pressure at the inlet and the exhaust systems and the %EGR if used. Information on the mass flow through the engine is desirable but not necessary in order to use the model. The number of zones, their AFR and mass fraction can be chosen arbitrarily and tailored to give the average NOx concentration that matches the measured.

The model consists of two parts. In the first part the heat release rate (HR) is calculated by using the geometrical properties of the engine, the inlet conditions and the pressure information. Different methods of computing the heat release rate were considered, but a method based on the first law of thermodynamics as described in [1] was chosen. This method is referred to as the ”single transducer method” in [2]. The HR model can be categorized as a diagnostic Zero-Dimensional model as discussed in [3]. The actual gas composition in the cylinder and the number of molecules are calculated in the second part of the model. The heat transfer model used is suggested by Woschni and described in [1]. The coefficients in the Woschni model are adapted by considering the calculated gross released heat, the amount of supplied fuel energy and the combustion efficiency given by the exhaust gas composition. This method is described in [4].

The HR calculations, i.e. the first part of the model, are based on the pressure measurements in the cylinder. It

can be shown that the errors in horizontal positioning of the pressure trace and phasing to the volume may have a detrimental effect on the calculated HR rate. In order to minimize these errors, methods proposed in [5] have been used.

In the second part of the model the HR rate is used to calculate the mass of fuel and air involved in combustion during each time step. The temperature and combustion product composition, including NO, in the combustion zone and in the product zones are calculated.

The model has some similarities with the phenomenological spray combustion model proposed by Hiroyaso [6] in the sense that it divides the combustion zone in packages. The main differences are that in this model the energy release at each time step is given by the HR calculation and the condition in each package is determined by the chosen lambda value. A package should not be looked upon as a specific volume but rather as the sum of all combusted volumes having the same air/fuel ratio.

In the present model the zone lambda values are put in more or less manually in the setup routine. In this regard it resembles the two stage model presented in [7] where one stage lambda is chosen to a value below the cylinder average and the other to a value above. However, in the model presented in [7] the combustion in the two stages does not take place simultaneously.

The model that is written in the MATLAB toolbox SIMULINK was verified by using measured NOx emission from a premixed natural gas engine.

Data from a direct injected stratified charge engine and a diesel engine were used to study the effect of injection duration on the average local lambda. During these calculations the ambition was to find the average local lambda that gave the same NOx emissions as measured at different injection periods.

The idea was to investigate the local lambda of the early phases of the combustion in direct injected engines. This study was triggered by the results from the conceptual combustion model presented in [8], where it is suggested that the premixed combustion takes place at extremely fuel-rich conditions.

The method of using heat release data and measured NOx emissions to estimate the local lambda during combustion is not new. In [9] the method is used to analyze the combustion conditions in the PREDIC (PREmixed lean Diesel Combustion) system.

The word ”zone” will be used with several meanings in the text below. To avoid confusion the following distinctions have to be given. A time zone is generated at every time step of calculation. It starts as a combustion zone when created and is labeled a post combustion zone in the next and following time steps. A time zone can be subdivided into lambda zones and the fractions with different lambda are maintained throughout the calculation. The zone generation logic is illustrated in Figure 9 below. The model presented in the paper is called a multizone model. This name refers to that fact that the post combustion zones are separated throughout the energy release

In the continuing project the diagnostic model presented in this paper will act as a support when using laser-based diagnostic methods on the combustion process in an optical diesel engine.

THE MODEL

A printout from MATLAB/SIMULINK showing the model from the top level is found in Figure 1 below. A decisive reason why MATLAB was chosen for the model was that this matrix-oriented language is very suitable when dealing with vectors like time series, i.e. the pressure traces and tables like the JANAF tables. Subroutines calculating the thermo-dynamic properties of the different mixtures of gases involved in the combustion process and NO formation are easily accomplished.

Another important reason for choosing the MATLAB toolbox SIMULINK was that the events going on in the cylinder are truly dynamic. As SIMULINK is developed for dynamic simulations a lot of built-in functions and symbols are available.

The boxes in the top row in Figure 1 are the HR part of the model. It consists of input and output sections and submodels for calculating the net heat release, the heat transfer, gross heat release and IMEP.

The box at the bottom row in Figure 1, ZONECOMB, is the submodel were the zones are generated, the combustion takes place and the properties in the post-combustion zones updated.

As can be seen in the figure below there is a feedback from the ZONECOMB box to the NetHR box in the HR model. The properties of the content of the cylinder have an impact on global quantities used in the HR calculation; thus the actual data has to be fed in to the NetHR model.

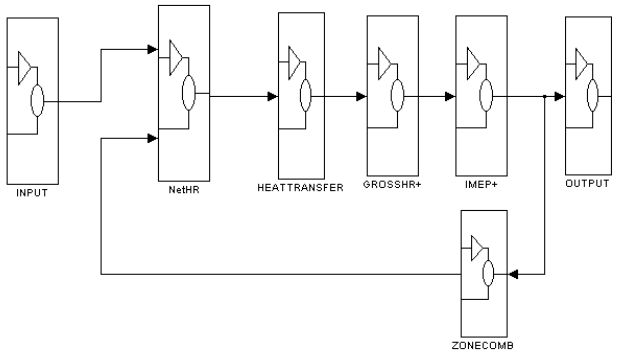

Figure 1. The general layout of the model

The program is initiated by a SETUP routine where the input files with the engine and pressure data are imported and initial calculations performed.

INPUT – In the input section the tables with time series of crank angle, pressure and other measured quantities from the engine tests are read. Options are given to change the phasing between the crank angle and the pressure and to offset the pressure curve horizontally.

The volume is calculated by using the crank angle information and geometrical data. Initially the SIMULINK derivation function was used to get the time derivative of pressure and volume, but it was found that this did not give a correct heat release rate during the later portion of expansion. The reason is probably that the SIMULINK function only uses the information from previous time steps to calculate a trend rather than a true derivative. For that reason a new derivation routine was developed where the benefit of knowing the whole time series was utilized. In this routine the step forward and backward could be chosen arbitrarily.

As pressure data from the natural gas engines was sampled every 0.2 CAD (in the diesel engine case: 1 CAD) the shortest CAD interval for derivation was 0.4 CAD. A comparison with this interval and an interval of 2.0 CAD gave a very small difference in the released heat, but the rate curve become smoother with the longer step.

Although the input data was given every 0.2 CAD the derivation and calculation steps in the INPUT section could be chosen arbitrarily by interpolation.

NETHR – The net heat release (Qn) is calculated by an expression derived from the first law of thermodynamics. Any effects of blowby, crevices and the enthalpy of the injected fuel (when applicable) are neglected.

$$\frac{dQn}{dt} = \frac{g}{g-1} p \frac{dV}{dt} + \frac{1}{g-1} V \frac{dp}{dt} \qquad \text{(Eq. 1)}$$

Where:

Qn is the net heat release [J]
g is the ratio of specific heats [-]
p is the pressure [Pa]
V is the volume [m^3]

For given pressure and volume input data the only variable in equation (1) is the ratio of specific heats γ. This parameter can be calculated in a number of ways. In this work three expressions have been evaluated. They are:

1. $g = kappa(GAS, T)$ (Eq. 2)
2. $g = g_0 - k_1 \exp(-k_2 / T)$ (Eq. 3)

where:

g_0 is a reference value [-]
k_1 and k_2 are constants [-]

3. $g = g_0 - K_1 (T - T_{ref}) / 1000$ (Eq. 4)

Where:

g_0 is a reference value [-]
K_1 is a constant [-]
T_{ref} is a reference temperature [K]

Kappa in the first expression is a MATLAB function that calculates γ for a given mixture of gases given by the vector GAS at the temperature T. Gas property data are taken from the JANAF tables or from [10]. The latter data are probably derived from the JANAF tables.

The different expressions 1-3 for calculating γ were evaluated by using the following input data:

GAS = Air/fuel mixtures with natural gas with lambda 1, 1.25, 1.50 and 2.0. Combustion products with lambda = 1.
g_0 = 1.38
k_1 = 0.2
k_2 = 900
K_1 = 0.08
T_{ref} = 300

The results from the γ-investigation are shown in Figures 2 and 3 below.

As can be seen in Figure 2 the different ways of calculating γ give different results. It can also be seen that the combustion products have higher γ than the air/fuel mixture. By choosing the constants carefully, expression 2 can give quite an accurate result over the entire temperature range, while expression 3 gives a good fit limited to a rather narrow temperature interval.

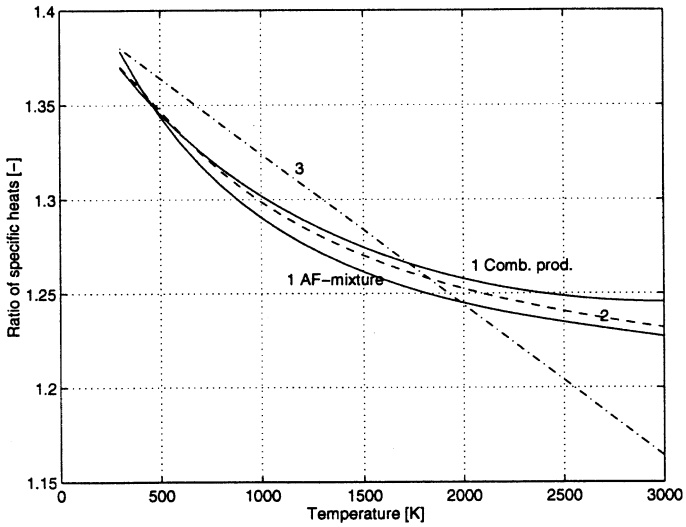

Figure 2. Ratio of specific heats calculated in three ways. The numbers refer to the expressions above. The gases used in expression 1 are the stoichiometric air/fuel mixture and the corresponding combustion products.

The ratio of specific heats is also influenced by the lambda value. This is shown in Figure 3 where the expression 1 is used for AF mixtures with lambda 1 to 2. At T=1500 K γ is increased by about 1.5 % in the studied lambda interval.

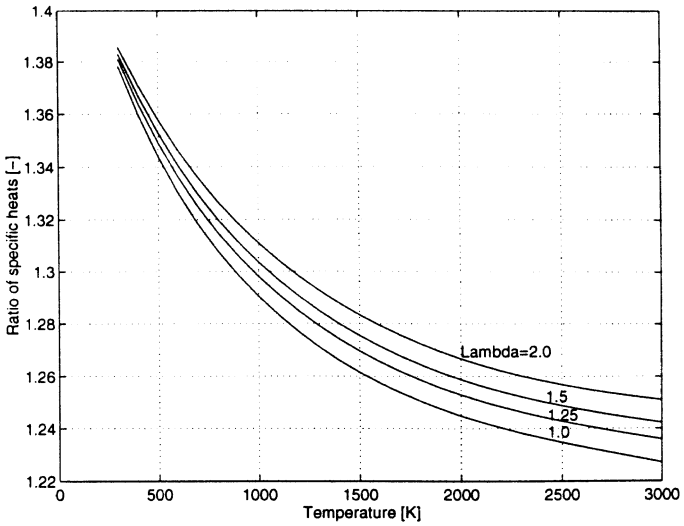

Figure 3. Ratio of specific heats calculated with expression 1 for four AF mixtures with different lambda values.

As the heat release calculations start at the end of the compression stroke, the need for accurate calculations of γ is limited to temperatures above about 800 K. The most critical temperature region, from the accuracy point of view, is where the heat release rate reaches its maximum. This happens when the average temperature increase during combustion has reached about half its maximum value. At lean combustion with lambda around 1.5 this occurs at a temperature level of 1500 - 1600 K.

The results from heat release calculations where expressions 1 - 3 are used are shown in the following three figures, 4 - 6. The data set used during these calculations, RUN_01, is found in Table 1.

The different γ-curves generated when performing a heat release calculation using data set RUN_01 are shown in Figure 4 below. The same constants as used in Figure 2 are applied.

The lambda in RUN_01 is 1.49, which means that the constants used to fit to lambda=1 in expression 2 give a too low γ-value all over the studied crank angle interval. It is then assumed that expression 1 using the actual gas composition gives the correct value.

Expression 3 seems to give γ-values that are far removed from the ones given by expression 1. However, when looking at the most important heat release interval 0 - 30 CAD the match with expression 1 data is not so bad. This is illustrated in Figure 5 that shows the heat release rate data.

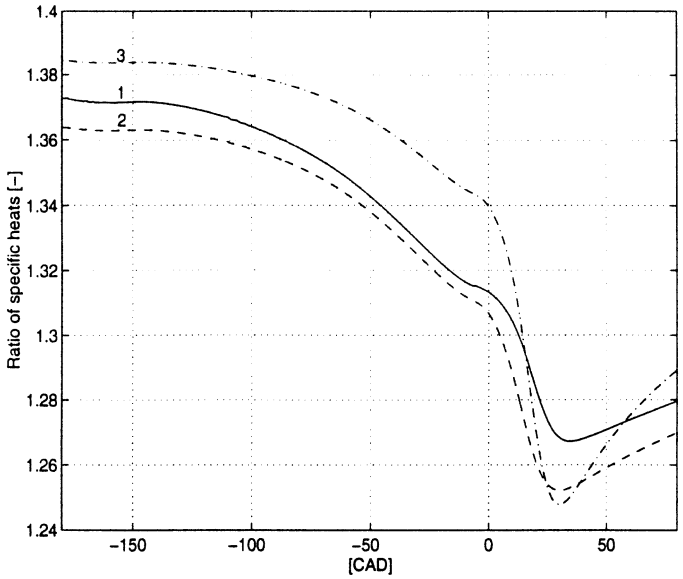

Figure 4. Ratio of specific heats calculated with expressions 1 - 3. Data set RUN_01.

A low γ-value gives a high rate of heat release. Thus, up to about 15 CAD $\gamma(2)$ (γ calculated with expression 2) gives the highest rate followed by $\gamma(1)$ and $\gamma(3)$. In the CAD interval 15 - 60 the rate with $\gamma(3)$ is higher than with $\gamma(1)$. In a small interval around 30 CAD $\gamma(3)$ is lower than $\gamma(2)$ and thus gives a higher rate.

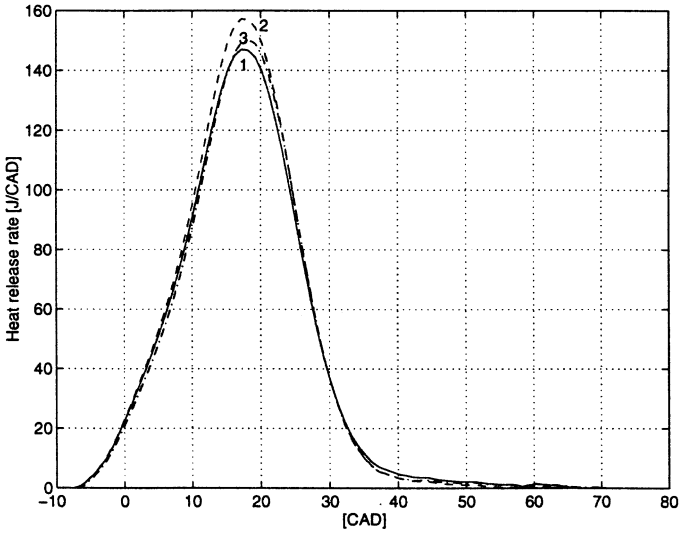

Figure 5. Calculated heat release rates for data set RUN_01 using three expressions for γ-calculations.

As $\gamma(2)$ gives the highest rate at the crank angle where the heat release reaches its maximum, the heat released calculated with expression 2 is about 3% higher than with expressions 1 and 3. This is illustrated in Figure 6.

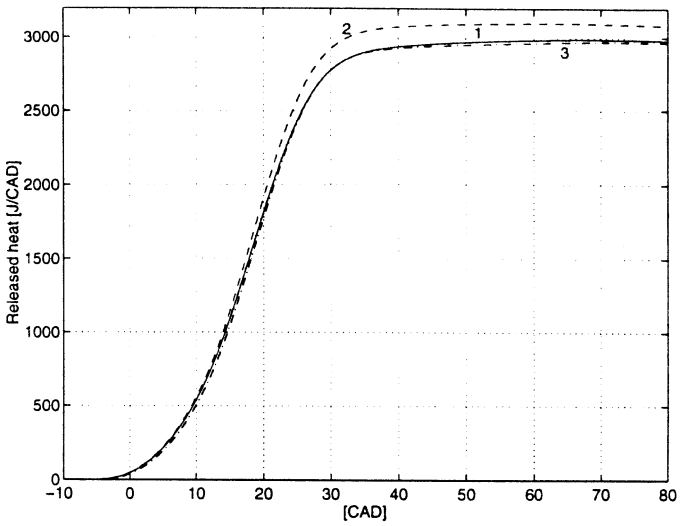

Figure 6. Released heat for data set RUN_01 using three expressions for γ-calculations.

The conclusion from examining different methods to calculate the ratio of specific heats is that it is possible to get a good match with ”correct” data with rather simple expressions, but then the constants have to be chosen carefully with respect to the influence of temperature and the gas composition. As this requires knowledge of the correct data it is better to use them in the first place.

HEAT TRANSFER – In order to establish the rate of combustion the heat flux to the walls has to be accounted for. In the present model only convective heat transfer is considered.

The standard expression for convective heat transfer is:

$$\frac{dQ_{ht}}{dt} = h_c \times Area_{wall}(T_{gas} - T_{wall}) \qquad \text{(Eq. 5)}$$

Where:

Q_{ht} is the heat transferred to wall by convection [J]

h_c is the heat transfer coefficient [W/K m^2]

$Area_{wall}$ is the area of the wall [m^2]

T_{gas} is the temperature of the gas [K]

T_{wall} is the temperature of the wall [K]

In order to use (5) the heat transfer coefficient h_c has to be estimated. For this purpose the expression proposed by Woschni and presented in [1] is used in the model.

$$h_c = 3.26 B^{-0.2} p^{0.8} T^{-0.55} w^{0.8} \qquad \text{(Eq. 6)}$$

Where:

B is the bore of the cylinder [m]

p is the cylinder pressure [kPa]

T is the gas temperature [K]

w is the average gas velocity [m/s]

w is calculated with the following equation:

$$w = [C_1 \overline{S_p} + C_2 \frac{V_d T_{ivc}}{p_{ivc} V_{ivc}} (p - p_m)] \qquad \text{(Eq. 7)}$$

where:

$\overline{S_p}$ is the mean piston speed [m/s]

V_d is the displaced volume [m3]

T_{ivc} is the temperature at inlet valve closing [K]

p_{ivc} is the pressure at inlet valve closing [Pa]

V_{ivc} is the volume at inlet valve closing [m2]

p is the cylinder pressure [Pa]

p_m is the motored cylinder pressure at the same crank angle as p [Pa]

C_1 = 6.18 at the gas exchange period
= 2.28 at the compression period
= 2.28 at the combustion and expansion period

C_2 = 0.0 at gas exchange and compression periods
= 3.24e-3 at the combustion and expansion periods

The constants C_1, and C_2 can be changed to fit h_c for a given engine. In the heat transfer calculations for the lean burn natural gas engine, i.e. RUN_01 to RUN_18 in Table 2, the constants have been multiplied by a factor of 0. The reason for this will be given below.

It is also possible to vary T_{wall} in (5) in order to tune the heat loss, Qht.

The calculated heat release and heat transfer rates for RUN_01 are shown in Figure 7. The corresponding accumulated heats are shown in Fig. 8.

GROSS HEAT RELEASE (QG) – The maximum heat transfer rate (dQht) is about 5% of the maximum heat release rate dQg, i.e. the sum of dQn and dQht. And the peak value is found at about 25 CAD, which is 5 CAD after the peak value of dQg and corresponds roughly to the CAD where the maximum average temperature is reached.

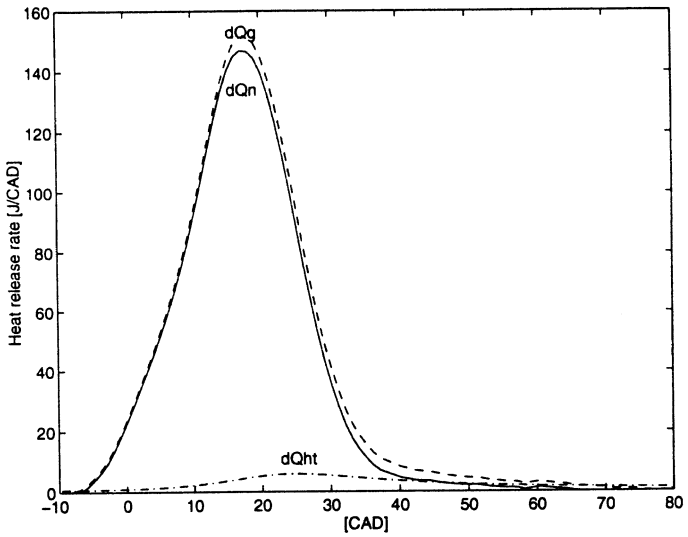

Figure 7. Heat release rates calculated for data set RUN_01. dQg=dQn+dQht.

The slope of Qn and Qg after about 25 CAD indicates that energy release is still going on very late during the expansion stroke. This could of course be due to the reverse dissociation reactions, but it is more likely that the parameter settings in the heat release model are not correctly tuned. In the calculations with data from the homogenous charge engine the heat transfer portion of Qg was omitted in order to get a more realistic shape of the heat release curve.

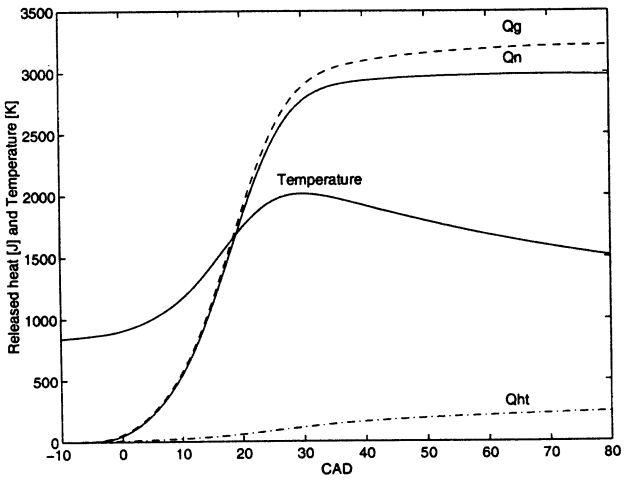

Figure 8. Temperature and released heat calculated for the RUN_01 data set. Qg=Qn+Qht.

TEMPERATURE – The temperature used in the heat release and heat transfer calculations, i.e. in equations (2) - (7) is given by the Ideal Gas Law:

$$pV = mRT \qquad \text{(Eq. 8)}$$

Where:

m is the mass in the cylinder [kg]

R is the gas constant [J/kg K] given by:

$$R = \frac{\tilde{R}}{M} \qquad \text{(Eq. 9)}$$

Where:

$\tilde{R}$ is the universal gas constant = 8314.3 [J/kmol K]

M is the molecular weight of the cylinder content

The Ideal Gas Law can also be written:

$$pV = n\tilde{R}T \qquad \text{(Eq. 10)}$$

$$n = \frac{m}{M} \qquad \text{(Eq. 11)}$$

Where: n is the number of moles

As the number of moles in the cylinder changes during combustion, the gas constant R is not constant, which in turn affects the calculated temperature. For that reason R is calculated at every time step using the actual number of moles; see the feedback from ZONECOMB to NetHR (where the temperature is calculated) in Figure 1.

The increase of moles during combustion when using natural gas is about 1.5% at lambda=1 and 0.5% at lambda=1.5. The temperature at given pressure and volume is lowered linearly with the increase of moles (10). The temperature affects γ and thereby the calculated net heat release Qn. The temperature also affects Qht and hence Qg.

As the temperature changes due to the increase of the number of moles are small, heat release calculations could very well by performed with a constant value of R. However, when calculating NO even a small change in the temperature could have a major impact on the result. For that reason the change of the number of moles is accounted for in the model.

MASS – For given values of the pressure p, volume V and the gas constant R the temperature scales linearly with the mass. See equation 8. A correct estimation of the mass of the cylinder content at inlet valve closing, IVC, is of decisive importance when calculating NO.

In the model this is done by calculating the number of residual gas moles, n_{res}, by using (10) at TDC during the gas exchange. If the fuel flow is not known the number of fuel moles, e.g. the supplied energy, is calculated by iteration until the fuel energy equals the maximum Qg while considering the combustion efficiency given by the measured concentrations of CO and THC in the exhaust.

The number of fuel moles, n_{fuel}, gives the number of air moles, n_{air}, as the average lambda value is known. When EGR is used, the number of EGR moles, n_{EGR}, can be calculated when the AF mixture is known. A preliminary calculation of the combustion products with the given lambda is performed to establish the molecular weight of the residual gas and the recirculated exhaust gas (EGR).

When knowing the number of moles in the charge and their weights, the mass in the cylinder can be calculated.

$$m_{ivc} = n_{air} M_{air} + n_{fuel} M_{fuel} + k_{res} n_{res} M_{res} + n_{EGR} M_{EGR} \quad \text{(Eq. 12)}$$

Where:

n_{nn} and M_{nn} are the number of moles and the molecular weight of nn.

k_{res} is a constant used for tuning the amount of residual gases in the charge. $k_{res} = 1$ means that the residual gases correspond to the mass in minimum volume of the cylinder at exhaust temperature and pressure.

IMEP – The indicated mean effective pressure is the work performed during a complete cycle normalized to the displacement volume. The work is given by:

$$W = \oint_{cycle} p \; dV \quad \text{(Eq. 13)}$$

$$IMEP = \frac{W}{V_d} \quad \text{(Eq. 14)}$$

IMEP is not part of the NO calculation but is convenient to use when checking the phasing of crank angle and pressure trace.

ZONECOMB – The tasks of this module are to:

1. Determine the energy released at each time step
2. Calculate the corresponding mass of fuel being burned
3. Split the mass in different lambda zones and calculate the corresponding charge of air, residual gases, and EGR. Determine the volume of the zone and the temperature.
4. Calculate the temperature and composition of the combustion products of each lambda zone.
5. Calculate the number of NO moles formed at the combustion of each zone.
6. Update the temperature and content of old lambda zones. And calculate the number of NO moles formed during the present time step in these zones.
7. Keep the record of the total number of moles, the number of NO moles, the volumes, temperaturesand species of all combusted zones and the temperature, moles and volume of the unburned charge.

A new zone at every preset lambda is generated at each time step during the combustion period. This means that the number of zones handled at the end of combustion is given by the number of lambdas and the number of time steps during combustion. To illustrate the zone generation logic consider the example shown in Figure 9 below.

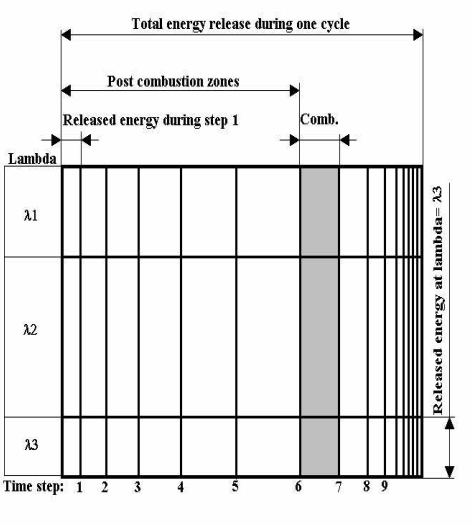

Figure 9. Definition of time and lambda zones.

In the figure above the total amount of energy released during one cycle is illustrated by the area of the rectangle. This energy is equal to the fuel energy released, i.e. the mass of fuel supplied times the lower heating value of the fuel. The fuel energy is corrected with the combustion efficiency that is calculated by using the exhaust gas composition. By tuning the coefficients C_1 and C_2 in equation (7) the heat transfer loss is tailored to give Qg the same value as the effective fuel energy.

When the fuel flow is not directly or indirectly given the procedure described on page 7 for MASS calculation is used to estimate the supplied fuel.

The areas between the vertical lines in Figure 9 represent the energy released at each time step and the area between the horizontal lines the energy released at a given lambda value.

Also shown in Figure 9 is a shaded area which illustrates the combustion zone at time step 7. In this case time zones 1 - 6 are post combustion zones and zones above 7 yet-unburned zones.

The number of zones to be stored in the memory is given by the equation below. Each zone is described by 14 scalars.

$$N = \sum_{i=1}^{n_{step}} n_{lambda} (n_{step} + 1 - i) \quad \text{(Eq. 15)}$$

Where:

n_{lambda} is the number of lambdas [-]

n_{step} is the number of time steps during combustion

Energy release – The energy released during the time step in question is given by the rate of heat release dQg times the length of the step.

The change of energy in the post- combustion zones, due to the change of composition (dissociation), is not accounted for when calculating the mass of fuel burned at each time step.

Lambda zones – The energy released during a time step is distributed in the chosen lambda zones according to the chosen proportions. The portion of the charge of air, residual gases and EGR corresponding to the mass of fuel and the given lambda is calculated for each lambda zone. In the example in Figure 9 the chosen lambdas are λ1, λ2 and λ3 and the proportions are illustrated by the size (height) of the corresponding areas.

The fuel mass involved is calculated by considering the efficiency of combustion, i.e. the content of CO and H_2 in the products (the combustion model does not give any unburned hydrocarbons). Thus, in zones with lambda < 1 more fuel than in a stoichiometric mixture is used to give the calculated energy release. This creates a conflict as the mass of fuel will be consumed before the total energy is released. However, it is assumed that the final oxidation of the combustion products from these zones will take place later during the expansion stroke and that these reactions do not contribute to the NO formation.

The temperature of the charge prior to combustion is calculated with the assumption that the change of conditions within the pre combustion zones is isentropic, i.e.

$$p_1 v_1^{g_1} = p_2 v_2^{g_2} \qquad \text{(Eq. 16)}$$

Where: p_i, v_i and g_i are the pressure [Pa], specific volume [m^3/kg] and ratio of specific heats [-].

By using the known conditions at the end of the compression stroke (before the start of combustion) and the pressure at the time step in question the specific volume of the unburned mass of the charge can be calculated by using (16). The γ - value from the previous time step is used. This is possible since the change of the temperature and thus γ is slow in the fresh charge. The volume [m^3] before combustion of the combustion zone in question is calculated, and then the temperature, by using the Ideal Gas Law (8).

In the diesel engine case the temperature in the considered combustion zone is reduced by the heat of vaporization of the fuel.

$$\Delta T_{vap} = \frac{m_{fuel} Q_{vap}}{m_{charge} Cp_{charge}} \qquad \text{(Eq. 17)}$$

Where:

m_{fuel} is the fuel mass in the combustion zone [kg]

Q_{vap} is the heat of vaporization of the fuel [J/kg]

m_{charge} is the total mass of the charge in the zone [kg]

Cp_{charge} is the specific heat at constant pressure [J/kg K]

Cp is calculated by using JANAF data for the mixture of gases in the charge. The heat required to heat the injected fuel to its boiling temperature is neglected.

Combustion – The mixture of gases including vaporized fuel, i.e. the reactants, in every lambda zone is considered homogenous, and the corresponding internal energy U_R is calculated by using JANAF data. The temperatures of the combustion products are calculated using an iteration loop where the volume, the work and the gas composition including the internal energy U_P are determined. The error in the energy balance is calculated and a new estimate of the product temperature is proposed. The method is described in [10].

The iteration process can be illustrated by the following equations:

1. The initial guess of the product temperature

$$T_p = T_R + \Delta T \qquad \text{(Eq. 18)}$$

Where:

$$\Delta T = f(Lambda, EGR) \qquad \text{(Eq. 19)}$$

The function f is manually adapted to the different conditions.

2. Initial guess for the composition and the number of moles of the combustion products. This guess is based on the lambda value in the zone in question.
3. The volume of combustion products is calculated using equation (10) slightly rearranged

$$V_P = \frac{n\tilde{R}T}{p} \qquad \text{(Eq. 20)}$$

4. The work is calculated using:

$$w = (V_P - V_R)\left(\frac{p_1 + p_2}{2}\right) \qquad \text{(Eq. 21)}$$

Where:

V_p is the volume of the products [m^3]

V_R is the volume of the reactants [m^3]

p_1 is the cylinder pressure before combustion [Pa]

p_2 is the cylinder pressure after combustion [Pa]

The pressures are given by the input pressure data at the crank angles in question.

5. The energy balance of the combustion zone assuming adiabatic combustion:

$$w = U_R - U_p \qquad \text{(Eq. 22)}$$

The error in the energy balance:

$$ERR = U_P + w - U_R \quad \text{(Eq. 23)}$$

6. New estimate of the product temperature

$$T_P = T_{P-old} - \frac{ERR}{C_v} \quad \text{(Eq. 24)}$$

Where C_v is calculated using JANAF data for the combustion products.

Dissociation – As the NO formation is strongly influenced by the temperature and the concentration of oxygen, it is necessary to take dissociation into account in the combustion model. This is done when calculating the composition of the products.

The combustion products considered are CO, CO_2, H_2, H_2O, O_2 and N_2. They are connected by the following reactions:

$$CO + H_2O \Leftrightarrow H_2 + CO_2 \quad \text{(Eq. 25)}$$

$$CO + \frac{1}{2}O_2 \Leftrightarrow CO_2 \quad \text{(Eq. 26)}$$

and the fact that each molecule of the oxygen in the air is accompanied by 3.773 molecules of nitrogen. All of the six species considered are present in the products, and the amounts of each (the number of moles) are given by the equilibrium constants K_{P1} and K_{P2} for (25) and (26) given in (27) and (28).

By increasing the temperature the equilibriums of reactions (25) and (26) are forced to the left, energy is stored and the temperature increase is limited.

$$\frac{P_{CO_2} P_{H_2}}{P_{CO} P_{H_2O}} = K_{P1} \quad \text{(Eq. 27)}$$

$$\frac{P_{CO_2}}{P_{CO}\sqrt{P_{O_2}}} = K_{P2} \quad \text{(Eq. 28)}$$

Where P_i is the normalized partial pressure of specie i.

The equilibrium constants can be calculated by the following expressions:

$$\Delta G^0 = -RT\ln(K_P) \quad \text{(Eq. 29)}$$

$$\Delta G^0 = \sum G^0{}_T \text{ (products)} - \sum G^0_T \text{ (reactants)} \quad \text{(Eq. 30)}$$

Where:

G^0 is the Gibbs free energy calculated by using data from the JANAF tables. With ”products” and ”reactants” are meant the species on the right and left sides in reactions (25) and (26) respectively

If the number of CO_2, CO, H_2O, H_2, O_2 and N_2 moles are named a_1, a_2, a_3, a_4, a_5 and a_6, equations (27) and (28) can be written:

$$\frac{a_1 a_4}{a_2 a_3} = K_{P1} \quad \text{(Eq. 31)}$$

$$\left(\frac{a_1}{a_2}\right)^2 \frac{1}{a_5} = \frac{P}{\sum_{j=1}^{6} a_j} K_{P2} \quad \text{(Eq. 32)}$$

When substituting the normalized partial pressures P_i

$$P_i = \frac{a_i}{\sum_{j=1}^{6} a_j} P \quad \text{(Eq. 33)}$$

Where P is the normalized total pressure

The number of atoms of the different elements in the products must equal the numbers in the unburned charge. Assuming that the fuel can be written C_nH_m and the combustion takes place at lambda=λ, the following equations must be valid:

Carbon balance:

$$n = a_1 + a_2 \quad \text{(Eq. 34)}$$

Hydrogen balance:

$$m = 2(a_3 + a_4) \quad \text{(Eq. 35)}$$

Oxygen balance:

$$2\left(n + \frac{m}{4}\right) l = 2a_1 + a_2 + a_3 + 2a_5 \quad \text{(Eq. 36)}$$

Nitrogen balance

$$2\left(n + \frac{m}{4}\right) l = \frac{a_6}{3.773} \quad \text{(Eq. 37)}$$

A nonlinear equation system of 6 equations is formed by (31), (32), (34), (35), (36) and (37). This system is solved with the MATLAB function fsolve.m for a given temperature, and the gas composition of the combustion products, i.e. a_1 - a_6, at that temperature is calculated.

Knowing the species of the products the internal energy, U_P, can be calculated by using JANAF data.

Post-combustion calculations – At every time step the contents of ”old” zones are updated. The temperature is changed due to changes in the pressure and the volume in the cylinder. The change of temperature effects the equilibrium constants and thus the composition of the products.

The calculations in the post-combustion zones are performed in the same manner as in the combustion zone. The temperature and species calculated in the preceding step are used as initial values.

Two Zone and Multi Zone models – In the basic model, i.e. the Multi Zone model, the combustion zone and the post-combustion zones are separated throughout the calculation and the NO formed in each zone is added to give the total amount of NO.

In order to study the consequences of separating the zones, a Two Zone model was developed from the Multi Zone model by adding the content of the combustion zone to a single post- combustion zone at every time step. The combustion zone was allowed to be one time step old before mixed with the post-combustion zone. Thus the NO contribution from the flame front was added to the total pool of NO. Tests were run without the addition of combustion zone NO and it was found that this contribution had a minor impact on the final result. In other words, most of the NO is formed in the post- combustion zones

NO – NO is calculated by using the Zeldovich mechanism:

$$O + N_2 \Leftrightarrow NO + N \qquad \text{(Eq. 38)}$$

$$N + O_2 \Leftrightarrow NO + O \qquad \text{(Eq. 39)}$$

Different expressions to calculate NO according to the Zeldovich mechanism are available in the literature. The following was found in [1].

$$\frac{d[NO]}{dt} = \frac{2R_1\left\{1-([NO]/[NO]_e)^2\right\}}{1+([NO]/[NO]_e)R_1/R_2} \qquad \text{(Eq. 40)}$$

Where:

$$R_1 = k_1^+[O]_e[N_2]_e \qquad \text{(Eq. 41)}$$

$$R_2 = k_2^-[NO]_e[O]_e \qquad \text{(Eq. 42)}$$

$[NN]_e$ is the equilibrium value of the specie NN .

$[N_2]_e$ is given by the (37)

$$[O]_e = \frac{K_{p(O)}[O_2]_e^{1/2}}{(\tilde{R}T)^{1/2}} \qquad \text{(Eq. 43)}$$

Where:

$[O_2]_e$ is given by (36) and

$$K_{p(O)} = 3.6e3\exp(\frac{-31090}{T}) \qquad \text{(Eq. 44)}$$

$$[NO]_e = (K_{NO}[O_2]_e[N_2]_e)^{1/2} \qquad \text{(Eq. 45)}$$

Where:

$$K_{NO} = 20.3\exp(\frac{-21650}{T}) \qquad \text{(Eq. 46)}$$

and k the rate constants for reactions (38 - 39). A "+" sign means the forward reaction.

k_1^+ =7.6e13 exp(-38000/T)

k_2^- =1.5e9 T exp(-19500/T)

In the combustion zone calculation only reaction (38) is used as [NO] << [NO]e. NO formed in the post-combustion zones is calculated considering both reactions, as [NO] in some zones comes close to [NO]e during certain conditions.

NO_2 – Nitrogen dioxide (NO_2) is not calculated in the model. As NO_2 is supposed to be formed from NO, the number of moles measured as NOx should equal the calculated number of NO moles. Thus, the calculated concentration of NO should match the measured concentration of NOx.

RESULTS

Data from a lean burn and a direct injection natural gas engine and a DI Diesel engine were used to evaluate the model. The lean burn data was utilised to test how well the model could predict NO in the premixed case where the local lambda equals the global.

The main objective of the analysis of DISC (Direct Injected Stratified Charge) and DI Diesel data was to establish the NOx based average lambda value in the combustion zones when the injection duration was varied. The theory was that the portion of NOx formed during the premixed combustion phase would dominate when the injection period was shortened. Thus the average lambda would be expected to increase when the injection period was reduced. If, however, the conceptual diesel combustion model presented in [8] is correct, the NOx based average lambda should vary little with injection duration as the premix combustion phase according to [8] does not contribute to the NO formation.

LEAN BURN (LB) ENGINE DATA – NOx measurements from an earlier project at the department were used to study NOx emissions from a homogenous charge LB engine. These data are published in [11] where details of the test engine and test conditions are also given.

In summary: the test engine was a converted diesel engine with a displacement of 1600 cm3. The bore was 121 mm and the stroke 140 mm. The combustion chamber used when producing the data utilized in this paper had a conical shape and a compression ratio of 13.5:1. Dimensions are given in Figure 10.

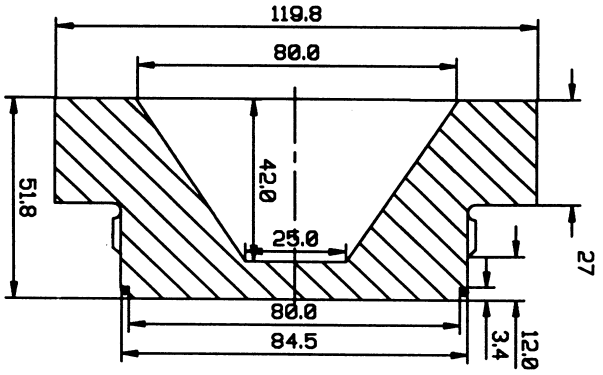

Figure 10. Geometry of the combustion chamber for the Lean Burn Engine

The variables during measurements were lambda, EGR and crank angle for ignition. Engine speed at all readings was 1200 rpm.

LEAN BURN ENGINE RESULTS – The measured and calculated NOx results from 18 runs are given in Table 1 below. The column labeled ”NOx” gives the measured NOx values. The label ”NO_M” marks the calculated NO concentrations from the Multi Zone model and ”NO_2” the corresponding data from the Two Zone model.

Table 1. Measured and calculated NOx/NO.Lean Burn.

RUN	Lambda	EGR	Ignition	NOx	NO_M	NO_2
	[-]	[%]	[CAD]	[ppm]	[ppm]	[ppm]
1	1.49	0.00	-11	419	714	693
2	1.49	0.00	-18	1248	1367	1217
3	1.61	0.00	-13	111	146	144
4	1.60	0.00	-22	581	647	555
5	1.71	0.00	-20	69	112	107
6	1.71	0.00	-25	195	225	197
7	1.79	0.00	-28	112	101	90
8	1.79	0.00	-32	202	197	155
9	1.01	8.30	-5	1405	2254	2269
10	1.01	8.48	-15	1704	2746	2878
11	1.01	10.80	-5	1217	1873	1871
12	1.01	10.80	-13	1525	2392	2456
13	1.01	18.10	-8	629	990	973
14	1.01	18.40	-16	1066	1397	1383
15	1.01	23.80	-14	363	537	527
16	1.01	23.90	-20	584	711	687
17	1.01	30.20	-26	179	211	203
18	1.01	30.10	-32	400	398	358

As can be seen both models give a good qualitative picture of the NOx emissions. The calculated values are higher than the measured in most cases, and the Multi Zone data are, with three exceptions, higher than the Two Zone values. The results are also shown in Figure 11 below.

During the LB calculations the effect of the heat transfer on Qg was neglected as this gave a cumulated heat release curve shape that probably corresponds better with the actual mass burning rate. By this assumption the calculated total energy supplied by the fuel became 5 - 10% too low. This in turn reduced the estimated mass of the charge at IVC. The mass flows were not measured in this case.

As will be demonstrated below the temperature at IVC had a major influence on the NO production. This temperature is inversely proportional to the mass in the cylinder at a given pressure. By using k_{res} in (12) as a variable in an iteration loop, the amount of residual gases was adapted to give the same number of moles in the cylinder at all runs. The same number of moles gave roughly the same mass and thus the same temperature as the pressure at IVC was almost constant for all runs.

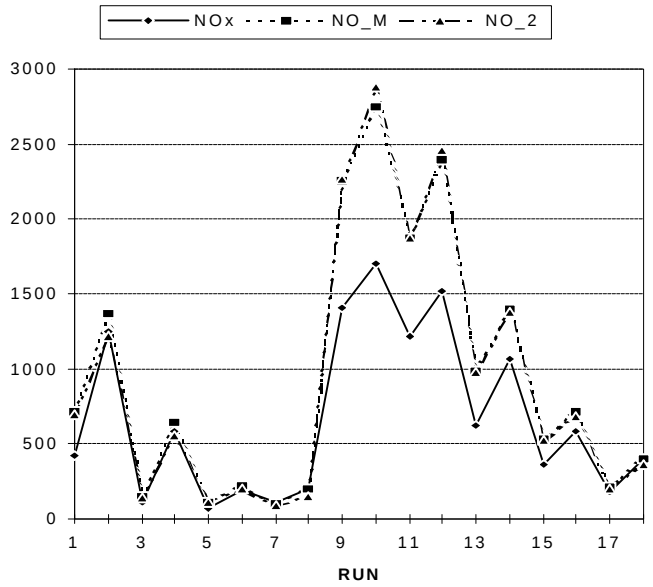

Figure 11. Measured and calculated NOx [ppm] versus RUN number. Lean Burn.

The results from RUN_04 and RUN_10 will be analyzed in some detail below. The RUN_04 is chosen because the calculated results are close to the measured and RUN_10 because of the fact that the Two Zone model gives higher NO than the Multi Zone.

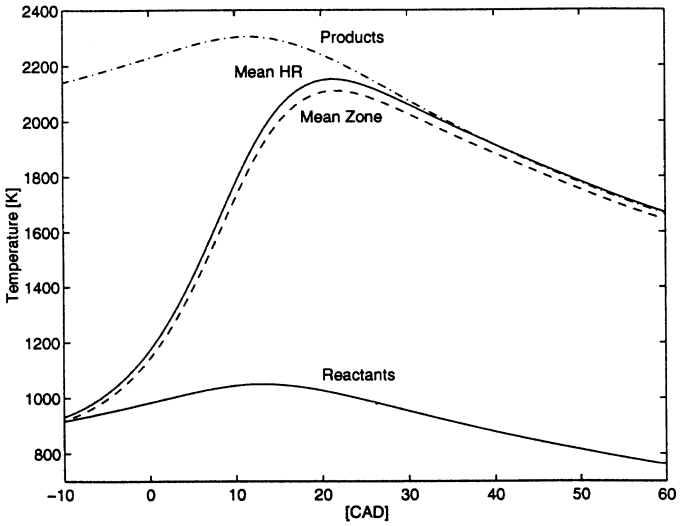

Figure 12. The temperature of products, reactants and the mean temperature calculated in two ways versus the crank angle. RUN_04.

The temperatures and volumes of each zone, including the unburned zone, are calculated without using the average temperature and the geometrical volume when the combustion has started. The accuracy of the zone model can therefore be judged by comparing the average temperature of all zones with the temperature given by the heat release portion of the model. For the same reason the sum of all zone volumes can be compared with the actual volume of the cylinder.

The temperature comparison for RUN_04 is shown in Figure 12, where the mean combustion product and the unburned charge (Reactants) temperatures are also included. As can be seen the mean zone temperature is slightly lower than the temperature calculated by (8).

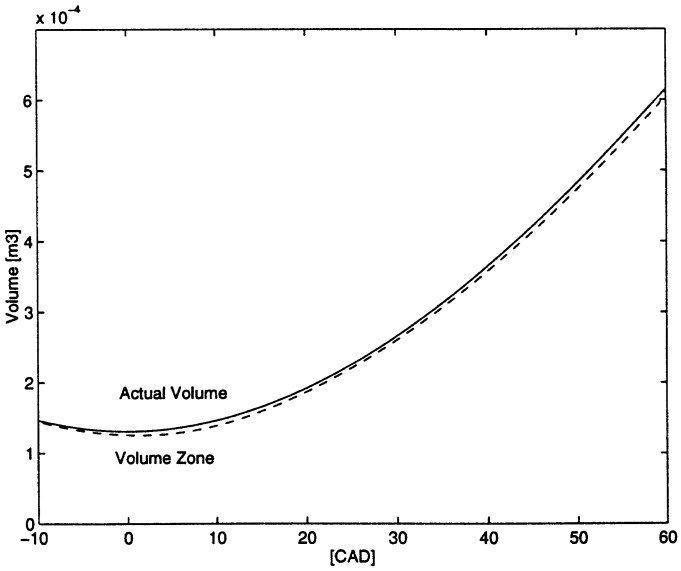

Figure 13. The sum of the calculated zone volumes and the actual cylinder volume versus the crank angle. RUN_04.

The sum of the zone volumes is lower than, but very close to, the actual volume of the cylinder as is shown in Figure 13.

The results from the NO calculations for RUN_04 indicate that calculated product temperature is a little too high. This is expected as combustion and post combustion zones are treated as adiabatic volumes. This means that the mean temperature calculated in the HR section by using the equation (8) is probably too high.

As was mentioned above the temperature of the charge at IVC has a major impact on the NO formation. This is demonstrated by data from RUN_04 in Figure 14. The calculated NO concentration is increased almost three times by a temperature rise of only 15 K. This demonstrates that, in order to use the model for quantitative calculations, it is necessary to have a very good estimation of the trapped mass or the temperature at IVC.

So far only average conditions and NO concentrations have been discussed. In the following figures the conditions in individual zones will be presented. The local temperatures in every third time zone are shown in Figure 15. The start point of every curve indicates at what crank angle the combustion of the zone in question took place. The highest temperature is reached in the first burned zone. After the combustion the temperature is further increased due to compression of the zone.

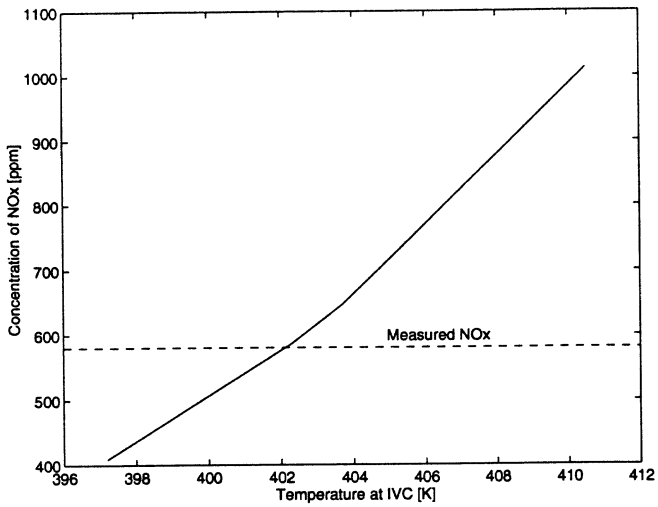

Figure 14. Calculated sensitivity of the temperature at IVC on NO formation. RUN_04.

The maximum local temperatures in RUN_04 are reached at about 13 CAD ATDC. This is about 7 CAD earlier than the maximum average temperature. See Figure 12.

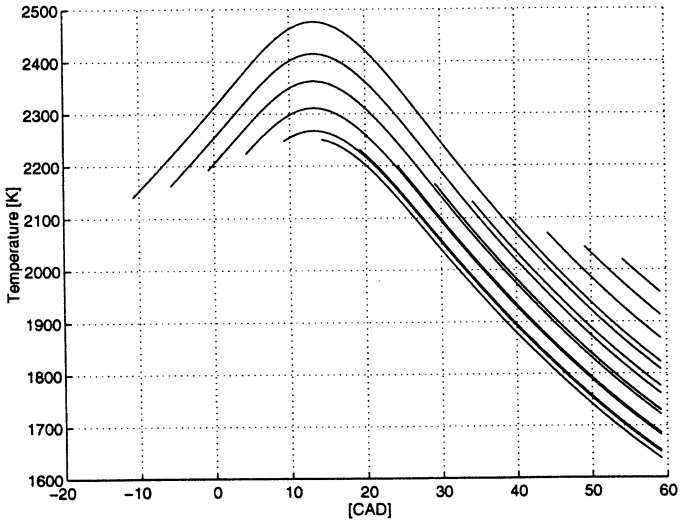

Figure 15. Local temperatures calculated with the Multi Zone model for RUN_04.

As expected, the local NO concentration in the first burned zone is the highest. This is shown in Figure 16. Considering that the average NO concentration is about 600 ppm the local value of about 5500 ppm is extremely high. Thus, when performing direct measurements of local NO concentrations, very steep gradients could be expected.

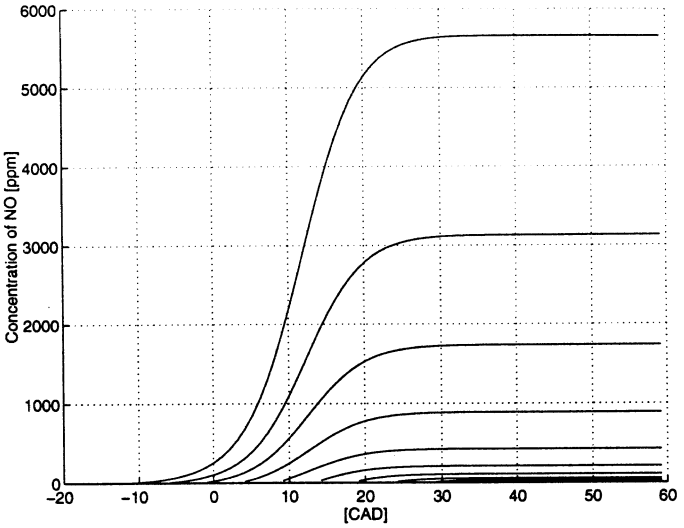

Figure 16. Local NO concentrations calculated with the Multi Zone model for RUN_04.

Although the NO concentrations in early burning zones are very high, these zones may not be the main contributor to total emissions of NO. This is a matter of how many moles of NO are produced within the zone in question.

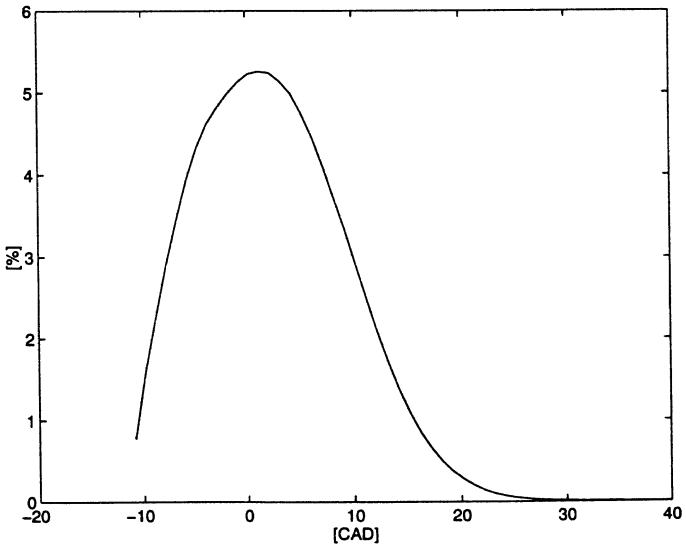

Figure 17. The calculated contribution to the total NO emission from zones with different burn angle. Histogram with steps of 1 CAD. RUN_04.

Figure 17 is a histogram with 1 CAD step where the contribution from zones with different burn angle to the total NO emission is demonstrated. As can be seen, zones that burn close to TDC are the biggest contributor to the NO emissions in RUN_04 according to the model.

In Figure 18 the global NO forming rate is compared with the gross heat release rate heat. The peek of NO formation is found at the location of the maximum local temperatures, i.e. 13 CAD ATDC in RUN_04.

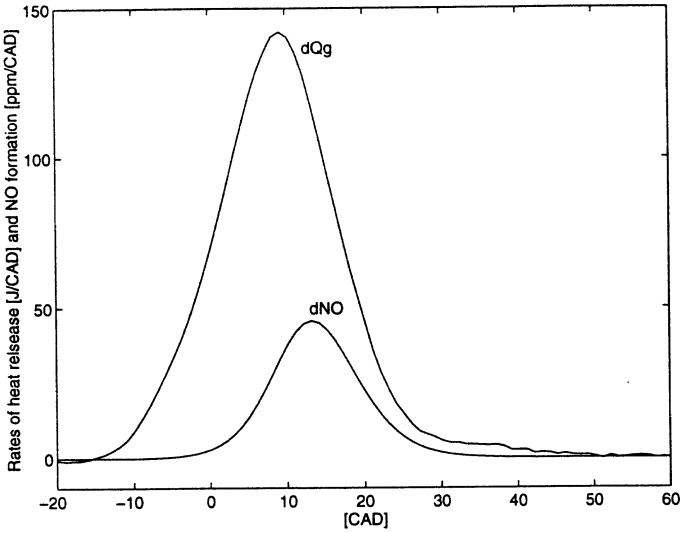

Figure 18. Calculated heat release and NO formation rates versus the crank angle. RUN_10

In looking for the explanation why the Two Zone model gives higher NO emissions than The Multi Zone in some conditions, the results from RUN_10 were investigated. When comparing the average NO formation rates from both models, see Figure 19, it can be seen that the peak value is about the same but the rate is higher at the right side of the rate curve with the Two Zone model.

The reason for this is found in Figure 20 that shows both local and average NO concentration for the Multi Zone case and local for the Two Zone case. The average product temperature of the Multi Zone calculation was only a few degrees higher than the local temperature in the Two Zone calculations. This somewhat surprising result is due to the dissociation in the high temperature zones according the model.

The NO concentration of the early burning zones in the Multi Zone calculations is declining at about 13 CAD ATDC. The levels are very close to the equilibrium values, and as this value is reduced with falling temperature (see equations (45) and (46)) the zone concentration has to follow. In the Two Zone case the NO production is not limited by the equilibrium value to the same extent, and the average concentration becomes higher. This can be seen by comparing the mean value of the Multi Zone results with the local concentration of the Two Zone model in Figure 20.

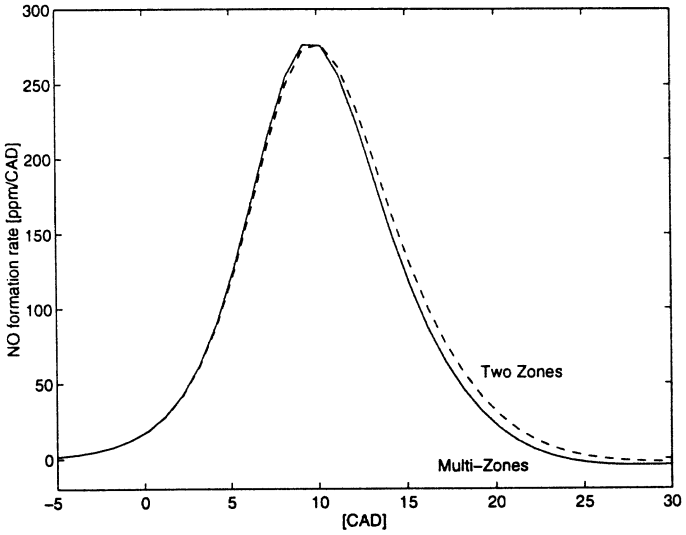

Figure 19. Calculated NO formation rates in the Two Zone and the Multi Zone models. RUN_10.

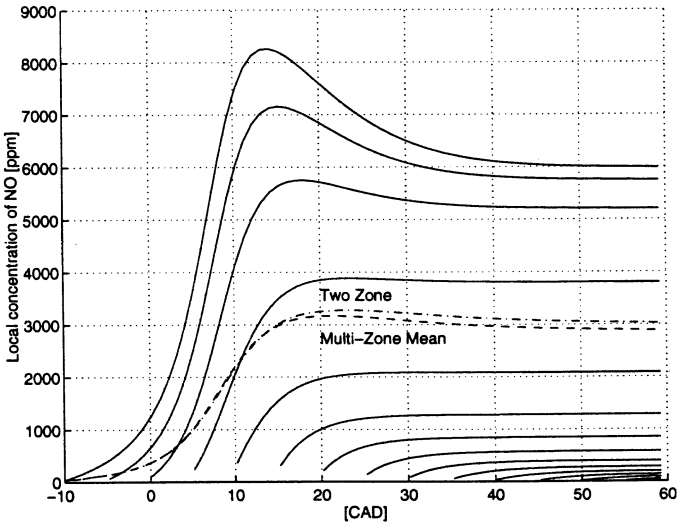

Figure 20. Calculated local and mean NO concentrations for the Multi Zone and the Two Zone models. RUN_10.

The results indicate that early burning zones with lambda close to 1 will have NO concentrations close to the equilibrium value.

Despite the simplifications, approximations and uncertainties in the model, the results from the analysis of the LB data shows that it is possible to calculate NO at different conditions with acceptable accuracy. This implies that the calculated local temperatures and concentrations of other species are also fairly correct.

DIRECT INJECTION STRATIFIED CHARGE (DISC) – The DISC engine measurements were run on the same engine as the LB experiments discussed above. However, the combustion chamber was changed and the cylinder head was equipped with an injector for natural gas. A cross section of the combustion chamber and the injector is shown in Figure 21. The compression ratio was 10.7:1. All readings were performed at 730 RPM. Details of the DISC engine and test results are found in [12].

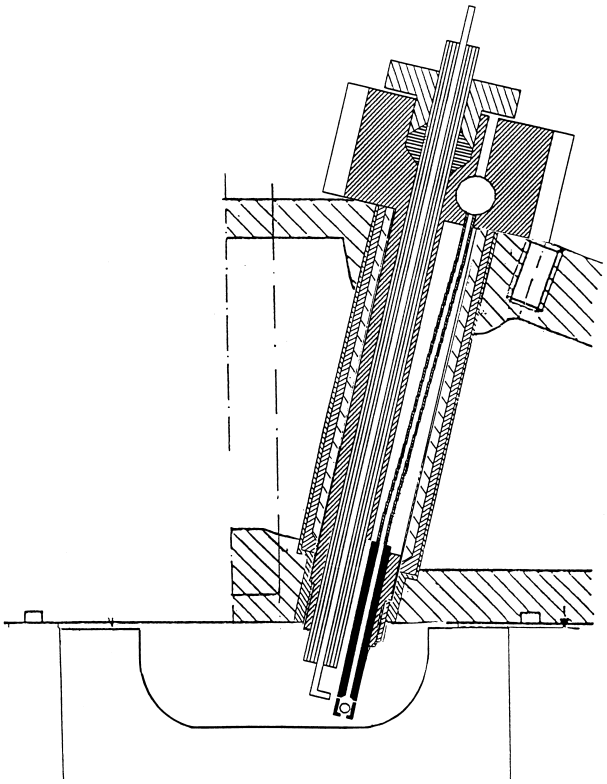

Figure 21. Cross section of the DISC engine combustion system

The start of injection was fixed at 60 CAD BTDC and the end of injection varied from 16 CAD BTDC to 71 CAD ATDC, giving the following injection durations: 44, 66, 88, 110 and 131 CAD. The spark was fired at 16 CAD BTDC. The idea was to gradually change the ratio between premixed and diffusive combustion and study the average local lambda determined by the Multi Zone model and the measured NOx emission. Measured quantities are gathered in Table 2 below.

The effect of varying the end of injection, i.e. the load, on the cylinder pressure trace is shown in Figure 22. As can be seen, about the same maximum pressure is reached in all cases. The main difference is the pressure level during the expansion stroke. The longer the injection period, the higher the pressure.

Table 2. Test results with DISC-combustion system and varied injection duration (DUR). Start of injection (SOI) 60 CAD BTDC. Average lambda = λ. Soot is measured with the Bacharach method.

EOI	DUR	λ	NOx	HC	CO	Soot
[CAD]	[CAD]	[-]	[ppm]	[ppm]	[%]	[-]
-16	44	9.3	28	1800	0.030	0
6	66	4.0	48	2000	0.121	4
28	88	2.4	58	1722	0.264	6
50	110	1.7	74	800	0.363	6
71	131	1.4	83	190	0.154	5

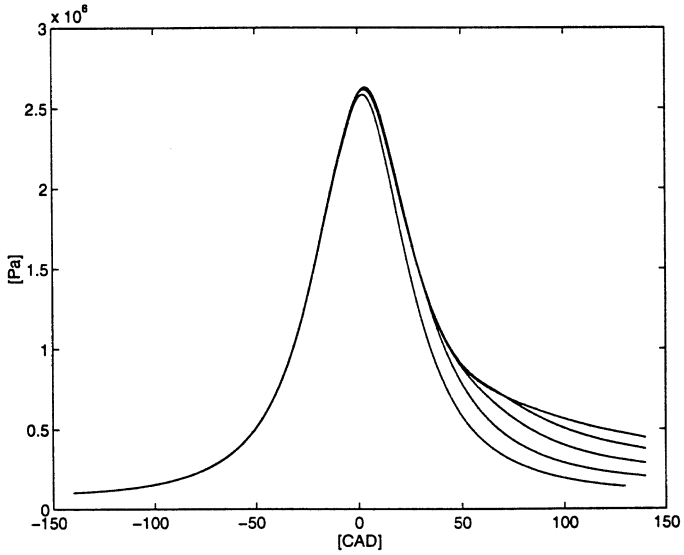

Figure 22. Measured pressure traces with varied injection duration.

The calculated heat release rates for the different durations are shown in Figure 23. The premixed and diffusive phases of the combustion are easily recognized.

It can also be seen that combustion takes place a long time after the injection has ended, which illustrates the diffusive character of the combustion

The NOx emissions in Table 2 are given in ppm. In order to connect the NOx formed to the fuel burned, the quantity emission index (EI) is calculated. EINOx has the dimension [g NOx / kg fuel].

The influence on EINOx of the injection duration is shown in Figure 24. As can be seen, the first portion of fuel injected contributes most to total NOx expelled. One reason for this is, as has been discussed above, that combustion products formed early have a longer residence time at high temperature levels and thus contribute more to the total NOx formed.

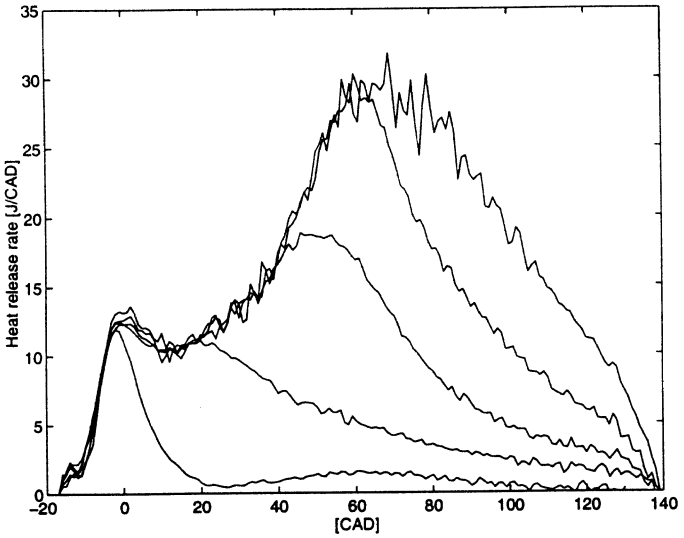

Figure 23. Calculated heat release rate with varied injection duration.

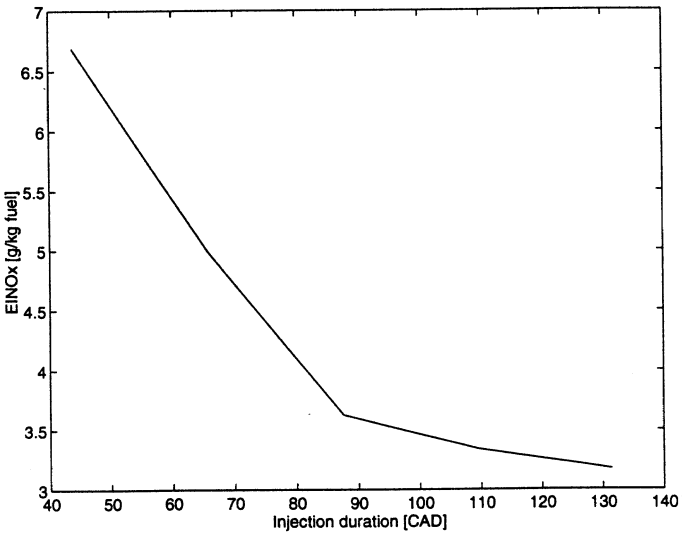

Figure 24. Measured EINOx versus Injection duration

Another reason could be that the portion of premixed combustion with higher lambda increases when the injection period is shortened. This theory is tested by using the Multi Zone model to find the average local lambda that gives the same calculated NO emission as the measured NOx concentration in the exhaust.

The resulting calculated average zone lambda values are shown versus injection duration in Figure 25.

It is also possible to find an average lean lambda that would give the same NOx emissions as measured. However, the high soot emissions, see Table 2, indicate that there exist very fuel rich areas within the combustion zone. For that reason it is believed that the average lambda is below 1. The very high HC emissions at the shortest durations is probably due to overleaning in the premixed portion of the charge.

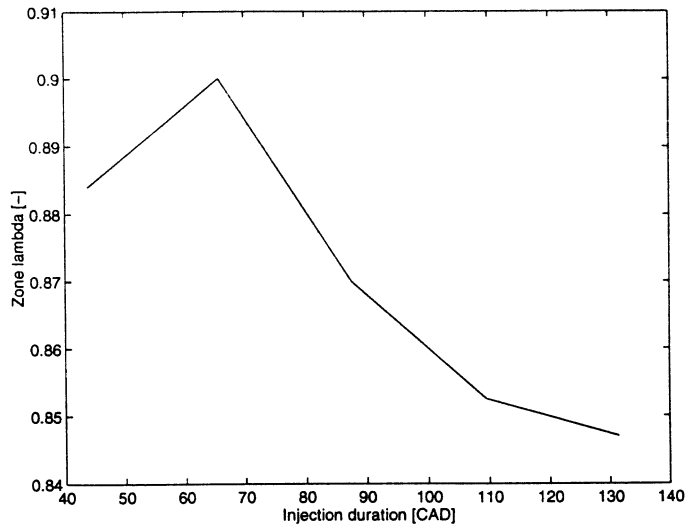

Figure 25. The calculated average local lambda that gives the same NOx emissions as measured versus injection durations.

The trend in Figure 25 is clear except for the shortest duration. The calculated local lambda is increasing with an early end of injection. However, one can not be sure that the degree of premixing, i.e. air entrainment, is the only reason for the calculated effect. At longer injection durations the residual gas temperature and thus the temperature of the charge at IVC increases. As has been demonstrated above the temperature at IVC has a decisive influence on the NO formation. This means that the calculated NO emissions at a given local lambda value increase with injection duration, and the local lambda has to be lowered to get a NO formation corresponding with the measured.

The effect of the increase of the charge temperature on NO formation can be seen in Figure 26. The figure shows the NO formation rate versus CAD at the different end of injections. Despite the variation of injection duration, NO formation peaks at slightly after TDC for all cases. However, the peak value increases with the duration. This could be due to the increased charge temperature. The calculated heat release rate around TDC shows the same trend. See Figure 23.

To summarize: The combustion situation in the DISC engine is very complex, which is reflected in the exhaust composition. At shortest duration injection stops at the same crank angle as the spark is fired. The mixture that is ignited is highly stratified and the first injected fuel is overleaned and gives very high emission of unburned hydrocarbons. The last injected fuel is not mixed with a sufficient amount of air and it is likely that some soot is formed. As the air excess is very high at this load the concentrations of soot will be low, which gives a low Bacharach reading. The high air excess will also promote soot oxidation during the expansion stroke.

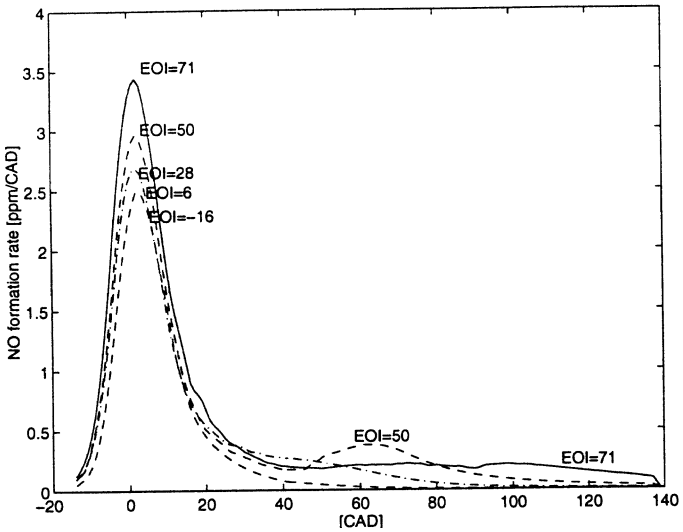

Figure 26. Calculated NO formation rate versus CAD for different end of injection.

The measured soot emissions at higher loads support the results from the calculations, i.e. the combustion takes place at very low lambda. The average lambda during the premix combustion could be very lean or very rich. However, the high soot emissions at the global lambda of 1.7 indicate that the combustion at this load takes place with fuel excess.

DI DIESEL – The diesel experiments were performed on a one cylinder supercharged heavy duty engine with a 2 liter displacement. The compression ratio was 18:1 and a common rail injection system was used. The engine speed was kept constant at 1200 RPM throughout the test.

Due to lack of JANAF data for diesel fuel, data for octane was used in the combustion and post- combustion calculations.

The start of injection (alfa) was fixed at 4 CAD before TDC and the duration was varied from 8 to 15 CAD. The corresponding average lambda values varied from 3.89 to 1.51. The needle lift curves for the different durations are shown in Figure 27. As can be seen, the motion of the needle starts some CAD before the set value for alfa. The needle lift during the shortest period (8 CAD) does not reach the same value as the rest. Some bouncing of the needle seems to occur at the end of injection.

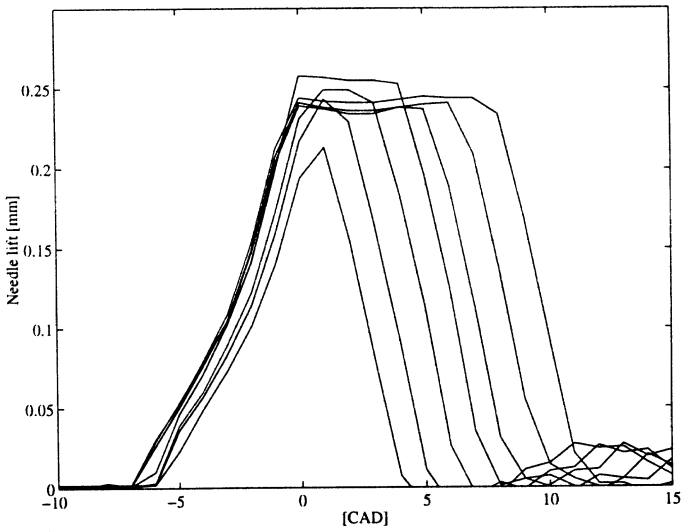

Figure 27. Measured needle lift versus CAD for injection period settings of 8, 9, 10, 11, 12, 13 and 15 CAD.

The pressure curves corresponding to the different injection durations are shown in Figure 28. As can be seen, the pressure prior to injection is almost constant. One concern, when the test series was planned, was that the conditions at the start injection would vary due to the different loads. This would in turn affect the ignition process and make it difficult to draw any firm conclusion about the influence of the duration as such. The pressure curves show that at least the pressure level at the start of injection is not affected to a great extent by the load.

The pressure data were used to calculate the heat release rate for the different injection periods. The resulting positive rates including the heat transfer loss, i.e. dQg, are shown in Figure 29. As can be seen, the rate at the beginning of the combustion period is about the same for all injection periods. When looking at Figure 29 one gets the impression that the ignition delay increases with the reduction of the duration. This is however not true. The variation in the start of the needle lift as a function of the duration is about the same order. See Figure 27. This means the time between the start of injection and the beginning of combustion is about the same for all injection durations. Thus, the change of load with different duration does not affect the ignition delay.

The measured NOx emissions given as emission index, EINOx [g NOx per kg fuel], decrease with the injection duration at the interval 11 to 15 CAD duration. At shorter durations the EINOx becomes less with reduced duration. Figure 30. The reason why EINOx declines at the lowest durations is probably the reduction at peak heat release rate. See Figure 29.

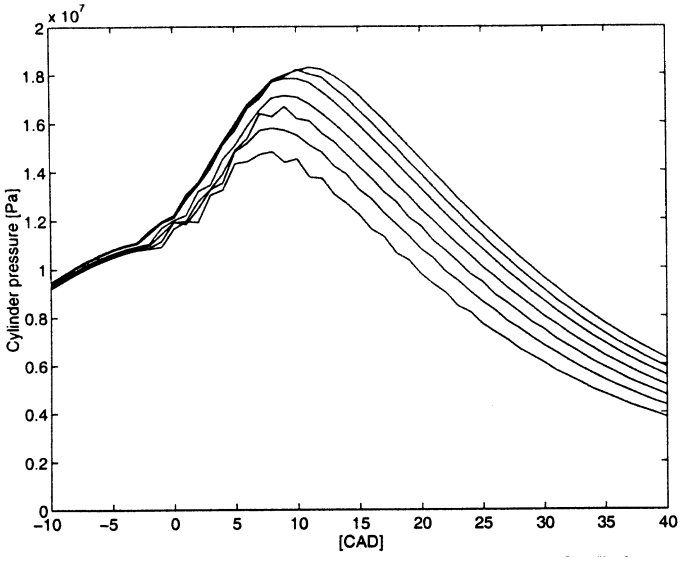

Figure 28. Measured cylinder pressure versus CAD for injection period settings of 8, 9, 10, 11, 12, 13 and 15 CAD.

The most interesting case, however, is the descent of EINOx with increasing duration above 11 CAD. There are two reasons why this would happen. Firstly: With a longer duration proportionally less fuel is involved in the most NO-producing zones. Secondly: Due to the pre-mixing during the ignition delay the lambda in the first portion of the fuel burned could be higher than the one in the following. Higher local lambda gives higher NO formation.

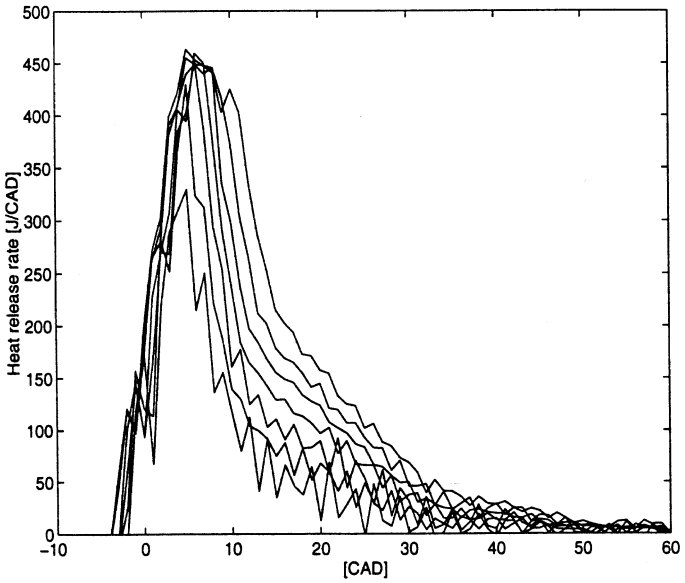

Figure 29. Calculated heat release rates versus CAD for injection period settings of 8, 9, 10, 11, 12, 13 and 15 CAD.

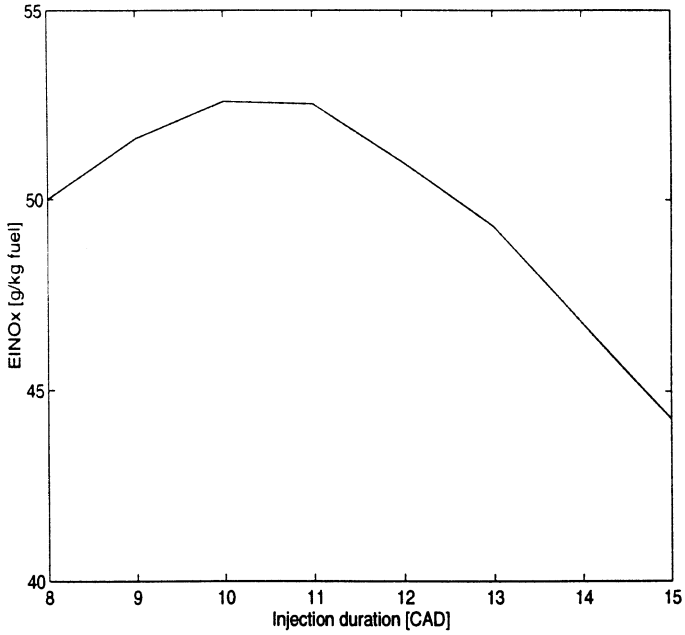

Figure 30. Measured EINOx versus Injection duration. Diesel data.

By using the Multi Zone model for NO formation, the effect of timing on the combustion of different quantities of the supplied fuel is accounted for. In order to analyze the possible effect of pre-mixing during the ignition delay, the average local lambda that would give the measured concentrations of NOx at the different injection durations was calculated by a manual iteration in the model. The result is shown in Figure 31.

As can be seen the average lambda in the combustion zones is slightly below 1 and increases with decreasing injection duration. This supports the theory that the initial combustion after the ignition delay takes place at a higher lambda than the following diffusive type combustion. It is then assumed that the lambda value at pre-mixed combustion is higher than at diffusive combustion. If this is not the case and the pre-mixed combustion takes place at such a low lambda that very little NO is formed, as suggested in [8], the results indicate that the local lambda during the diffusive portion of the combustion is slightly higher in the beginning that at the end.

The level of the calculated local lambda, i.e. slightly below one, seems to be realistic considering the nature of the diffusive combustion.

The calculated NO formation rates at the different injection durations are shown in Figure 32. The peak value is increasing with the duration and the location of the peek is slightly delayed. The peak position of NO formation corresponds quite well with the crank angle of maximum heat release rate. See Figure 29.

The analysis based on NO formation shows that the combustion on average takes place at close to the stoichiometric conditions. In order to estimate the potential of increasing the air entrainment in the spray, some calculations with higher lambda values were performed at the full load condition, i.e. injection duration 15 CAD. The result is shown in Figure 33 where EINOx is given as a function of lambda for the given heat release rate.

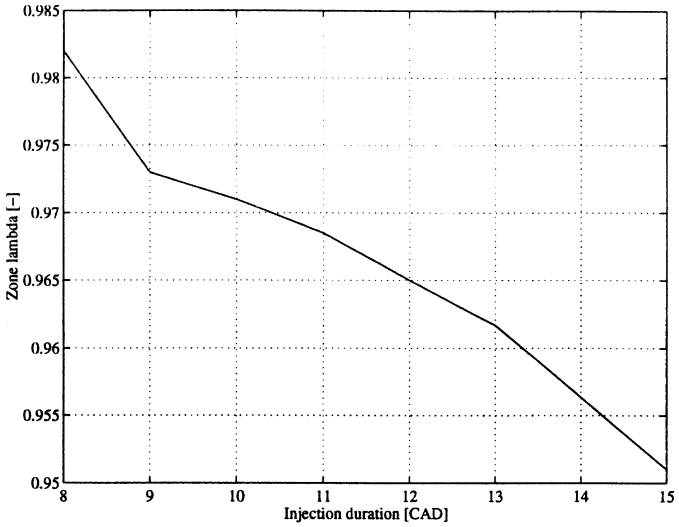

Figure 31. The calculated average local lambda that gives the same NOx emissions as measured versus injection duration.

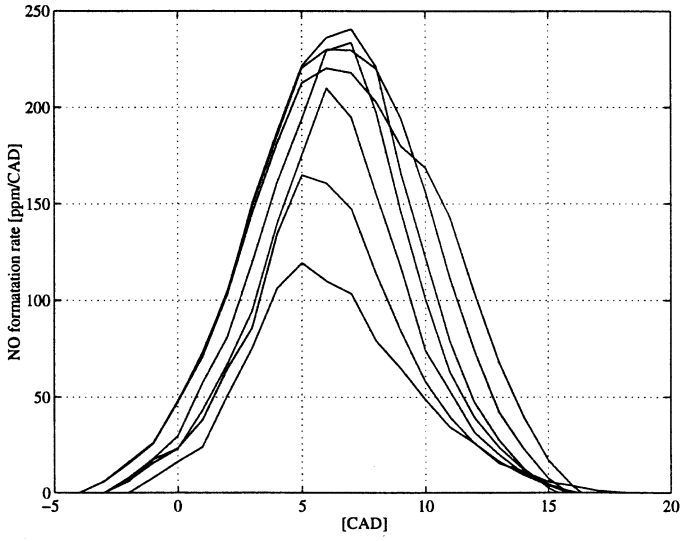

Figure 32. Calculated NO formation rate versus CAD for injection period settings of 8, 9, 10, 11, 12, 13 and 15 CAD.

The conclusion from this calculation experiment is that it is not possible to reduce the NOx emissions by increasing the air entrainment at this load. At lambda = 1.5, which is the average lambda, EINOx is still higher than the measured value which was achieved at local lambda=0.95.

In the real case the heat release rate would probably be affected by the increase of lambda and the NOx emissions lower than shown in Figure 33. On the other hand the slower heat release would also have a negative effect on the fuel consumption.

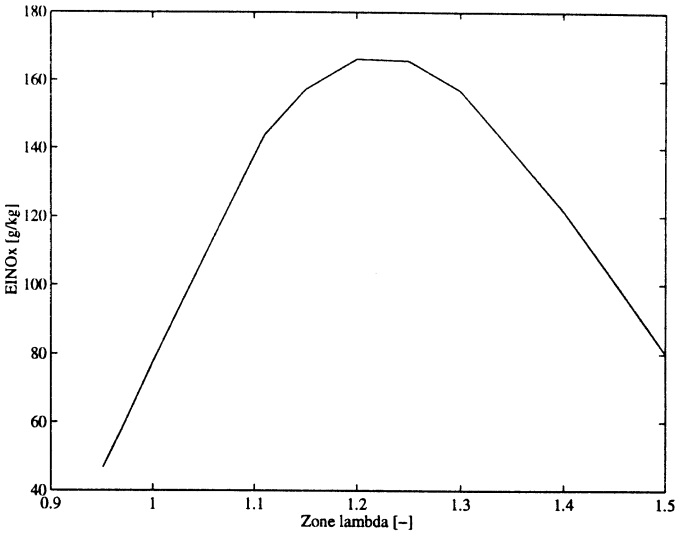

Figure 33. Calculated EINOx versus local lambda at a given heat release.

DISCUSSION

It must be pointed out that the presented model is not a diesel combustion model. It is rather an extension to common heat release analysis techniques for direct injected engines. Measured NOx emissions are used as a tool to calculate local conditions. It is only in the homogenous charge cases that the model could be applied to predict NOx emissions.

Although the model is designed for combustion in multiple lambda zones the results presented in this paper are derived from calculations with only one lambda value, i.e. the average local lambda. This is of course a modest ambition, but one has to keep in mind that it is generally believed that diffusive combustion takes place in a rather narrow band close to the stoichiometric air/fuel rartio. Finding the average lambda value in that band is the first step in creating a possible lambda distribution within initial diffusive combustion zone.

In the next version of the program the lambda distribution will be given by probability density functions (PDFs) according to a method presented in [13]. These functions can be changed in the post- combustion zones in order to simulate changes in air entrainment and mixing between zones. The final goal is to express the properties of a given spray by time-dependent PDFs.

Additional information on the lambda distribution can be extracted from soot measurements, but the final confirmation must be found by direct measurements in an engine.

The NO model is presently based on the mechanism originally proposed by Zeldovich, i.e. the third reaction in the extended Zeldovich mechanism is neglected. How this simplification affects the calculated average local lambda is not known to the author at the moment, but it is believed that the calculated lambda value would be slightly increased if the extended mechanism is used.

SUMMARY AND CONCLUSIONS

A multizone model for combustion diagnostics based on heat release and NO calculation has been developed. The model is used as an analytical tool where measured NOx emissions and other parameters available outside the engine are utilized to estimate the local conditions during combustion. In the continuing project the model will act as a support when using laser-based diagnostic methods on the combustion process in an optical diesel engine.

One new lambda zone of each local lambda is generated and the temperature, volume and species in all old zones are updated at each time step of calculation. In this paper the model is demonstrated by using pressure data from pre-mixed and direct injected stratified charge natural gas SI engines and from a DI diesel engine.

The pre-mixed data is used to validate the model as such while the ambition in the stratified charge and diesel cases has been to find the average local lambda at combustion that gives the same NOx emission as measured. The emphasis in the latter cases has been to study the influence on average local lambda of the duration of the fuel injection.

It was found when using pre-mixed data that the model gives a good qualitative picture of NO formation during various combinations of lambda, ignition angle and EGR rates. A good quantitative agreement was reached at higher lambdas and EGR rates. At close to stoichiometric AFR with small amounts of EGR, the calculated NO concentration was up to 70% too high. The reason for that could be that the combustion and post combustion zones were treated as adiabatic volumes. The calculated temperature would then be too high.

The results form the pre-mixed calculations indicate the local concentration of NO in early burning zones could reach close to the equilibrium values. This was also found to be the reason why a two zone model, in some conditions, could give higher NO emissions than the multizone model.

According to the results the gradients of NO in the combustion products could be very high. Early burning zones could have NO concentrations several orders of magnitudes higher than late burning zones.

Another observation was that the mass in the cylinder at inlet valve closing had a dramatic effect on NO formation in the model. At a given pressure and volume the temperature of the charge is inversely proportional to the mass. Thus, a change in trapped mass gives the corresponding change of the temperature at IVC. The NO formation in the model was extremely sensitive to the temperature of the unburned charge. A 15 K increase of the temperature at IVC in the temperature resulted in more than double the NO concentration.

The analysis of DISC (Direct Injection Stratified Charge) and diesel data showed that diffusive type combustion seems to occur at slightly fuel-rich conditions. The DISC data suggests an average lambda in the range of 0.85 - 0.90. The corresponding calculated range for diesel combustion was 0.95 - 0.98. The reason why the diesel engine combustion takes place at higher lambda than the combustion in the direct injected natural gas engine could be better penetration of the liquid diesel spray.

The highest average local lambdas at initial combustion for both engines were found at short injection periods. A possible explanation is that the portion of pre-mixed combustion increases with the reduced injection time. It is then assumed that the lambda value at pre-mixed combustion is higher than at diffusive combustion. If this is not the case and the pre-mixed combustion takes place at such a low lambda that very little NO is formed, as suggested in [8], the results indicate that the local lambda during the diffusive portion of the combustion is slightly higher in the beginning that at the end.

At the highest load with the diesel engine the average lambda, i.e. calculated with supplied air and fuel, was 1.51. The calculated average local lambda during combustion at this load was 0.95. In order to investigate the NO reduction potential by increasing the air entrainment at a given heat release, NO was calculated for the lambda range 0.95 - 1.51. It was found that even at the highest lambda NO was still higher than the measured. Thus, under the given conditions increased mixing of fuel and air would give higher NOx.

ACKNOWLEDGMENTS

The author would like to thank Scania CV AB for supplying the measured data for the diesel engine. The project has been financed by the National Council for Technical Research and Vehicle Engineering. The author is very grateful for this support.

Warm thanks are also directed to Bengt Cyrén at Aspen Utvecklings AB for his contribution of MATLAB routines for calculation of thermodynamic properties of species.

REFERENCES

1. Heywood, J. B. ”Internal Combustion Fundamentals” McGraw-Hill series in mechanical engineering. 1988.
2. Grimm B. M. and Johnson R.T. ”Review of Simple Heat Release Computations” SAE Paper 900445. 1990
3. Foster D.E. ”An Overview of Zero-Dimensional Thermodynamic Models for IC Engine Data analysis”. SAE Paper 852070. 1985
4. Homsy, S.C. and Atreya, A. ”An Experimental Heat Release Rate Analysis of a Diesel Engine Operating Under Steady State Conditions”. SAE Paper 970889. 1997.
5. Callahan T.J., Yost, D.M. and Ryan III, T.W. ”Acquisition and Interpretation of Diesel Engine Heat Release Data” SAE Paper 852068. 1985
6. Yoshizaki, T., Nishida, K. and Hiroyasu, H. ”Approach to Low NOx and Smoke Emission Engines by Using Phenomenological Simulation”. SAE Paper 930612. 1993.
7. Szekely Jr, G.A. and Alkidas, A.C. ”A Two-Stage Heat-Release Model for Diesel Engines” SAE Paper 861272. 1986
8. Dec, J.D. ”A Conceptual Model of Diesel Combustion Based on Laser-Sheet Imaging” SAE Paper 970873. 1997
9. Nakagome, K., Shimazaki, N., Niimura, K., and Kobayashi, S. ” Combustion and Emission Characteristics of Premixed Lean Diesel Combustion Engine”. SAE Paper 970898. 1997
10. Benson, R.S. and Whitehouse, N.D. ”Internal Combustion Engines.” Volumes 1 and 2 Pergamon Press. 1979
11. Olsson K., Johansson, B. ”Combustion Chambers for Natural Gas SI Engines. Part 2: Combustion and Emissions”. SAE Paper 950517. 1995
12. Egnell, R. ”Impact of Combustion Chamber Geometry on Charge Stratification in a CNG Fueled Direct Injection Otto Engine”. ISRN LUTMDN/TMVK—7016-SE. 1994 Department of Heat and Power Engineering Lund Institute of Technology
13. Kobayashi, H., Kamimoto, T. and Matsuoka, S. ”Prediction of the Rate of Heat Release of a Axisymmetrical Diesel Flame in a Rapid Compression Machine”. SAE Paper 840519. 1984